


Article

Experimental Study for Improving the Repair of Magnesium–Aluminium Hybrid Parts by Turning Processes

Eva María Rubio ^{1,*} , María Villeta ², José Luis Valencia ² and José Manuel Sáenz de Pipaón ¹

¹ Department of Manufacturing Engineering, Industrial Engineering School, Universidad Nacional de Educación a Distancia (UNED), St/Juan del Rosal 12, E28040 Madrid, Spain; jm@saenzdepipaon.com

² Department of Statistics and Operation Research III, Faculty of Statistical Studies, Complutense University of Madrid (UCM), Ave. Puerta de Hierro 1, E28040 Madrid, Spain; mvilleta@estad.ucm.es (M.V.); joseval@estad.ucm.es (J.L.V.)

* Correspondence: erubio@ind.uned.es; Tel.: +34-913-988-226

Received: 23 November 2017; Accepted: 11 January 2018; Published: 16 January 2018

Abstract: One of the lightest metallic materials used in the aeronautics, aerospace, and automotive industries, among others, is magnesium, due to its excellent weight/strength ratio. Most parts used in these industries need to be made of materials that are rigid, strong, and lightweight, but sometimes the materials do not simultaneously satisfy all of the properties required. An alternative is to combine two or more materials, giving rise to a hybrid component that can satisfy a wider range of properties. The pieces machined in these industrial fields must satisfy stringent surface roughness requirements that conform to the design specifications. This work shows an experimental study to analyse the surface roughness reached in hybrid components made up of a base of magnesium alloy (UNS M11917) and two inserts of aluminium alloy (UNS A92024) obtained by turning. Its purpose is to determine the influence of the factors and their possible interactions on the response variable, the surface roughness Ra . The study is carried out using a design of experiments (DOE). A product of a full factorial 2^3 and a block of two factors 3×2 was selected. The factors identified as possible sources of variation of the surface roughness are: depth of cut, feed rate, spindle speed, type of tool, location with respect to the specimen (*LRS*), and location with respect to the insert (*LRI*). Data were analysed by means of the analysis of variance (ANOVA) method. The main conclusion is the possibility to carry out the repair and maintenance of parts of magnesium–aluminum hybrid components by dry turning; that is, without cutting fluids and, therefore, in the most sustainable way that the process can be carried out. In addition, different combinations of cutting parameters have been identified that allow these operations to be carried out in an efficient manner, reducing mechanization times and, therefore, also the direct and indirect costs associated with them.

Keywords: hybrid components; magnesium; aluminium; repair and maintenance operations; dry turning; mean roughness average (Ra); ANOVA

1. Introduction

Industries such as aerospace, aeronautics, and automotion need to reduce the weight of their vehicles in order to be able to transport more passengers and/or goods, to have a greater range of action, or to reduce fuel consumption.

One way to achieve weight reduction in vehicles is to use lighter components made of light alloys (usually aluminium, titanium, and/or magnesium) having excellent weight/strength ratios. Most parts of the industries mentioned above, in addition to being made of lightweight materials, have to be rigid, strong, and meet high requirements of precision and quality. Sometimes, the available

materials do not simultaneously satisfy all of the properties required, so that the design of parts in these fields has to adopt balanced decisions which do not satisfy one or more of the mentioned properties. The traditional method to improve the performance of the materials is the development of new alloys or polymers that increase the number of application areas, but this development may be expensive and not always achievable. An alternative is to combine two or more materials that already exist, giving rise to a hybrid component whose properties can satisfy a broader range than those of the materials, which conform to it, separately.

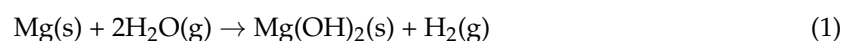
The requirements of the aerospace, aeronautical, and automotive industries, which are constantly searching for materials that cover a larger number of properties with the most recent technological advances, have generated a great demand for new materials or combinations of existing metals.

In recent years, these industries have opted for the use of hybrid components that combine their properties and may cover part of the property areas not covered by the individual components [1,2]. Many studies have been carried out to analyze the possibilities and limitations of different technologies to weld dissimilar materials [3–6]. It has been shown that a suitable selection method may result in a combination of materials that meet the mechanical requirements without a cost penalty [7].

In the aviation sector, hybrid components have been used in building the fuselage and wings [8] plus sandwich structures, where sheet metal and composite materials are used [9,10]. In the automotive field, they have also conducted studies on the combination of different materials, such as aluminium and steel [11], aluminum and titanium [11,12], as well as metal and composite [13–16]. Hybrid components, such as aluminium pistons with steel inserts to improve its functionality [17], have also appeared. Among the combinations of materials that just have been shown (steel, light alloys, and composites), those which have been attracting more attention in recent years are those having magnesium as a base [18]. In fact, studies have been conducted to analyze the possibilities and limitations of combining it with aluminium [19,20], titanium [20], or steel [20–23]. An application of these combinations is given in the manufacture of motor vehicles, where magnesium alloy is used in engine blocks, aluminium on cylinder liners, and sintered steel in the seats of crankshafts [24,25].

Additionally, due to the complexity and cost of most parts used in the manufacture of an aircraft, they have to be repaired for re-use. Then, for carrying out repair and maintenance operations on them, it is necessary to extract them from the set, which means that the whole aircraft will stop working and, therefore, will not produce benefits for as long as the individual parts are being maintained or repaired. Therefore, it is important to perform maintenance or repair activities of such parts as efficiently as possible, reducing replacement time and costs, which are both directly associated with the repair of the part as those are derived from the whole set not being in service [20]. Hence, performing machining operations in complex geometries of hybrid components is a significant challenge in terms of accuracy and quality; in particular, components based on magnesium, due to the heat generated during the machining process, creates a risk to the safety of the process [26,27].

Magnesium has the tendency to ignite, a trend that increases when machining in the presence of other materials, such as steels, that produce sparks for cutting speeds from 200 to 300 m/min [26]. The use of water-based coolants is not recommended when machining magnesium alloys, since, in the case of chips on fire, magnesium decomposes water, forming hydrogen atmospheres that are highly explosive (Equation (1)) [28–31].



This could be solved by developing lubricants or coolants compatible with this type of material; however, its use is an additional expense to the process and a source of pollution. In recent years, attempts have been made to develop cheaper manufacturing technologies compatible with the environment, such as machining with a minimum quantity of lubricant (MQL), dry machining, or machining with cold compressed air [32,33]. Machining hybrid components causes an increase in the instability of the process, mainly due to the different cutting characteristics of the different materials [20].

The search for optimal combinations of cutting conditions, tools, and lubrication/cooling systems for the simultaneous machining of materials with different natures has been the subject of many investigations. They have analysed aspects such as cutting tools (base materials, geometry, coatings, and wear), the surface quality required for the optimal performance of the piece, and the lubrication system [20,26,27,30–39] or machining conditions used [40–44].

Following this line, a broad research project was proposed in which different geometries and material combinations were used in the manufacture of specimens of hybrid parts [20,45] (see Figure 1). The idea was to study separately the different simple geometries of bases and inserts, as well as different combinations of materials, that would establish, first, what was the geometry of the most suitable specimens for each of the processes to be analysed: turning, milling, and drilling; second, the best combinations of cutting parameters to perform repairs or maintenance operations of such types of simple parts; and, finally, to define new specimens that allow us to approach the more complex real hybrid parts upon which new trials would be made.

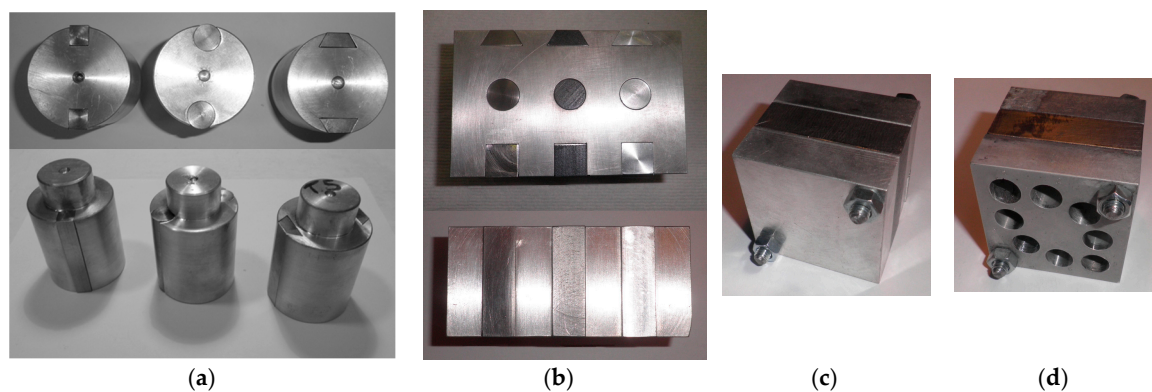


Figure 1. Hybrid part specimens with different geometries and combinations of materials for trials of: (a) turning; (b) milling; (c) drilling; and (d) repair and maintenance of holes by drilling.

This paper shows a particular case of the turning process whose goal is to determine the best combinations of cutting conditions, the type of tool to carry out the maintenance or repair of a hybrid part in the shortest time, and in the most sustainable way possible. Concretely, a specimen of a hybrid part with a magnesium base and two aluminium inserts with rectangular sections is analysed.

2. Methodology

The methodology used in this work follows the guidelines shown in Montgomery [46] and includes the following activities:

- Pre-experimental planning. Factors, levels, ranges, and response variables are set up.
- Selection of the experimental design. At this stage, the most adequate design of experiments (DOE) is selected according to the available resources and the objectives fixed in the study. In this case, the goal is to analyze the variability of the surface roughness of hybrid parts with a UNS M11917 magnesium alloy base and with two UNS A92024 aluminium alloy inserts obtained by turning. The surface roughness has been chosen as a response variable and, specifically, the arithmetic mean deviation of the assessed profile, R_a , because it is one of the most widely used variables in the literature and it allows for a better comparison with other studies on this theme. The process is to be performed with different types of tools, different cutting conditions, and under dry conditions, so that the potential influential factors to include in the design have been identified as: depth of cut, d ; feed rate, f ; spindle speed, S ; and type of tool, T . In addition, the R_a values are taken on different zones of the workpieces, since previous studies [47–53] have found that the location where the surface roughness measurement was taken seemed to influence

the value of the surface roughness. Now, there are two positions where the response variable is measured in the specimen: the location with respect to the specimen, *LRS*, and the position where the response variable is measured with respect to the insert, *LRI*. Their levels are fixed, taking into account the following criteria:

- First, the work is framed within a study involving other types of hybrid parts based on magnesium, but using different types of materials for the inserts used. Then, it seems reasonable to try, at least, two types of tools: one that is suitable for magnesium and other non-ferrous alloys, and another for other types of materials. Thus, it could be known how these tools behave with these materials and with others separately, to see if they can then be used in applications involving all types of materials. That is, two levels should be established for the factor, type of tool, *T*.
- Second, as the study deals with repair and maintenance operations, in general, the depth of cut, *d*, has to be as small as the available machines allow, since, otherwise, the parts could be out of dimensional tolerances. Then, one level is enough.
- Third, for the factors feed rate, *f*, and spindle speed, *S*, which are expected to have influences on the study (in particular the feed rate), two levels for each one are fixed.
- Finally, as has been mentioned above, previous studies seem to indicate that the roughness can vary with the length of machining of the piece. Therefore, *LRS* and *LRI* are going to be taken into account as influencing factors. Specifically, two levels for *LRS* and three levels for *LRI* will be established. That is, surface roughness measurements will be taken: for *LRS*, following the feeding direction, at the beginning of the specimen, *LRS1*, and at the end of the specimen, *LRS2*; and for *LRI*, according to the turning direction, before the insert, *LRI1*, in the insert, *LRI2*, and after the insert, *LRI3*. Table 1 shows the factors and levels fixed for them and their designations.

Table 1. Factors and levels.

Factors	Levels
Feed rate, <i>f</i> , (mm/rev)	<i>f1, f2</i>
Spindle speed, <i>S</i> , (rpm)	<i>S1, S2</i>
Type of tool, <i>T</i>	<i>T1, T2</i>
Depth of cut, <i>d</i> , (mm)	<i>d1</i>
Location with respect to the specimen, <i>LRS</i>	<i>LRS1, LRS2</i>
Location with respect to the insert, <i>LRI</i>	<i>LRI1, LRI2, LRI3</i>

With all of the considerations indicated until now, the experimental design selected is the product of a full factorial 2^3 and a block of two factors 3×2 . This aims to determine the influence of the factors and their possible interactions on the response variable. The design, once randomized in order to reduce the influence of not-considered variables on the results [46], has been collected in Table 2.

- Performing the experiment. As this work is framed within a larger project, the execution of the tests has been programmed to be carried out systematically following the next steps:
 - Previous activities to the machining process. These activities consist in preparing: the specimens of the hybrid parts, the tools, the protocols to be used to calculate the cutting parameters' values that will be introduced into the machine, the instrument where the surface roughness measurements will be taken, and the protocols to register the obtained data.
 - Turning trials. During the trials, specimens are mechanized under the cutting conditions determined for them.

- Monitoring processes. All of the turning trials described previously along with the obtained chips and used tools were photographed and recorded by video with a Hero Silver 4 high-resolution camera (GOPRO Inc., San Mateo, CA, USA) in order to have graphical documents that can be analysed once the process has finished.
- Roughness measurement. Measurements of the surface roughness are made using a Mitutoyo SurfTest SJ 401 surface roughness tester (Mitutoyo America Corporation, Aurora, IL, USA).
- Statistical analysis of the data. The statistical methodology carried out in order to analyze the results of the experimental design is briefly described in [54]. The variability of the surface roughness is modelled through the analysis of variance (ANOVA) over the average roughness values, Ra , identifying the most influential factors and interactions on the surface finish. The model hypothesis is checked, and the ranking of the different combinations of the process parameters' levels is obtained based on the roughness values predicted by the model. The optimal combination of cutting conditions (minimum expected roughness) is selected from such ranking. In addition, we conduct an exploratory data analysis to obtain a clear graphical view of the key aspects in the distribution of the influential factors on the surface finish of hybrid magnesium–aluminum parts, and relationships between pairs of influential factors have been illustrated by interaction graphs.
- Conclusions. Some conclusions are established from the results obtained in the statistical analysis.

Table 2. Randomized experimental design product of a full factorial 2^3 and a block of two factors 3×2 .

<i>T</i>	<i>S</i> , (rpm)	<i>f</i> , (mm/rev)	<i>LRI</i>	<i>LRS</i>		Observations
<i>T1</i>	<i>S1</i>	<i>f2</i>	<i>LRI2</i>	<i>LRS1</i>	<i>LRS2</i>	1
			<i>LRI1</i>	<i>LRS1</i>	<i>LRS2</i>	2
			<i>LRI3</i>	<i>LRS1</i>	<i>LRS2</i>	3
<i>T1</i>	<i>S1</i>	<i>f1</i>	<i>LRI3</i>	<i>LRS1</i>	<i>LRS2</i>	4
			<i>LRI2</i>	<i>LRS1</i>	<i>LRS2</i>	5
			<i>LRI1</i>	<i>LRS1</i>	<i>LRS2</i>	6
<i>T1</i>	<i>S2</i>	<i>f1</i>	<i>LRI2</i>	<i>LRS1</i>	<i>LRS2</i>	7
			<i>LRI1</i>	<i>LRS1</i>	<i>LRS2</i>	8
			<i>LRI3</i>	<i>LRS1</i>	<i>LRS2</i>	9
<i>T2</i>	<i>S1</i>	<i>f1</i>	<i>LRI3</i>	<i>LRS1</i>	<i>LRS2</i>	10
			<i>LRI2</i>	<i>LRS1</i>	<i>LRS2</i>	11
			<i>LRI1</i>	<i>LRS1</i>	<i>LRS2</i>	12
<i>T2</i>	<i>S2</i>	<i>f2</i>	<i>LRI3</i>	<i>LRS1</i>	<i>LRS2</i>	13
			<i>LRI2</i>	<i>LRS1</i>	<i>LRS2</i>	14
			<i>LRI1</i>	<i>LRS1</i>	<i>LRS2</i>	15
<i>T1</i>	<i>S2</i>	<i>f2</i>	<i>LRI3</i>	<i>LRS1</i>	<i>LRS2</i>	16
			<i>LRI1</i>	<i>LRS1</i>	<i>LRS2</i>	17
			<i>LRI2</i>	<i>LRS1</i>	<i>LRS2</i>	18
<i>T2</i>	<i>S1</i>	<i>f2</i>	<i>LRI1</i>	<i>LRS1</i>	<i>LRS2</i>	19
			<i>LRI2</i>	<i>LRS1</i>	<i>LRS2</i>	20
			<i>LRI3</i>	<i>LRS1</i>	<i>LRS2</i>	21
<i>T2</i>	<i>S2</i>	<i>f1</i>	<i>LRI1</i>	<i>LRS1</i>	<i>LRS2</i>	22
			<i>LRI2</i>	<i>LRS1</i>	<i>LRS2</i>	23
			<i>LRI3</i>	<i>LRS1</i>	<i>LRS2</i>	24

3. Experimental Tests

Within the larger project shown above, this work is focused in the manufacturing process of turning. In the following, the materials, cutting tools, cutting conditions, and measurement locations established as influencers of the surface roughness are going to be shown.

3.1. Materials

The materials used in the manufacturing of the trial specimens were, for the base, UNS M11917 magnesium alloy and, for the inserts, UNS A92024 aluminium alloy. The main reasons for selecting these materials were the following:

- In the absence of standards, national or international, or any other reference in relation to the design and fabrication of test pieces of metal hybrid components, such as those presented in this work, it was decided to start the study with different simple geometries for both the base and for the inserts, since, on many occasions, the repair and maintenance operations are limited to a small area of the surface of the piece and, therefore, the geometry to be machined is reduced to simple forms, such as those proposed in the general project regardless of the overall complexity of the piece [20,45]. On the other hand, this approach would allow, if necessary, for an increase in the degree of complexity of the geometry of the test pieces from solid knowledge about the joint behaviour of the individual materials depending on the results that were obtained.
- We have previous experience in the machining of both materials, both in continuous turning (horizontal and facing) [47–60] and in intermittent turning [56–60]. The geometry of the specimens raised in the present study is a natural evolution of the geometries and materials previously studied separately that have just been mentioned.
- In addition, the selected materials, both independently and jointly, have been used by other researchers in different investigations with good results in the field of study [61–71].
- The geometry of the specimen [45] (Figure 2) and the composition of these alloys (Table 3) are shown below.

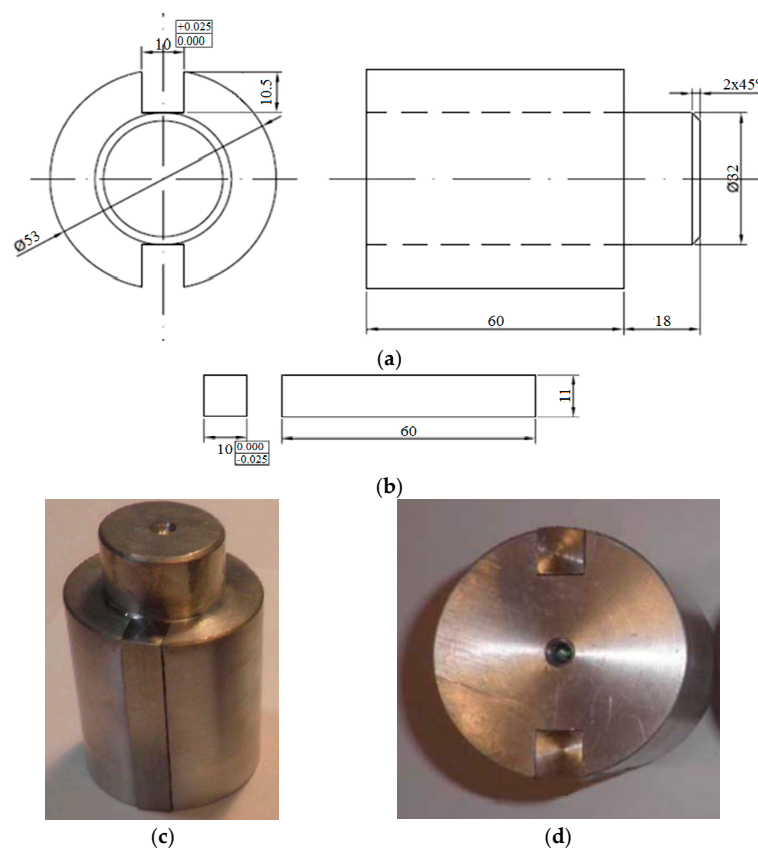


Figure 2. (a) Design of the UNS M11917 magnesium alloy base of the hybrid part specimen; (b) design of the UNS A92024 aluminium alloy insert of the hybrid part specimen; (c) turning specimen used during trials; and (d) detail of the specimen transversal section.

Table 3. Chemical composition of materials used for the manufacturing specimens.

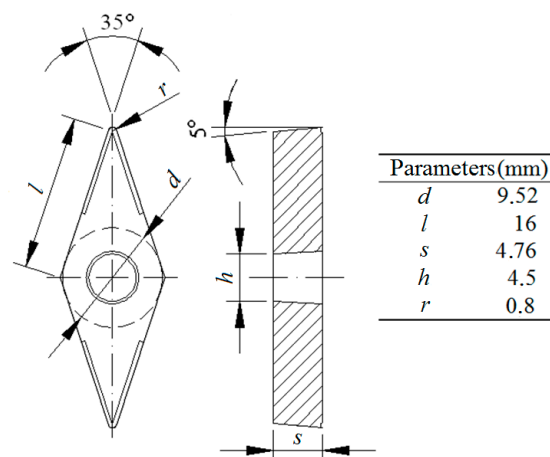
UNS M11917 (AZ91D)	UNS A92024 (AA2024 T351)
Al 8.30–9.70%	Al 90.7–94.7%
Cu \leq 0.03%	Cr \leq 0.1%
Fe \leq 0.005%	Cu 3.8–4.9%
Mg 90%	Fe \leq 0.5%
Mn \geq 0.13%	Mg 1.2–1.8%
Ni \leq 0.002%	Mn 0.3–0.9%
Si \leq 0.1%	Si \leq 0.5%
Zn 0.35–1%	Ti \leq 0.15%
-	Zn \leq 0.25%

The union of the inserts to the base was designed to be adjusted. However, for improving the security during the machining trials, where the specimens were going to be subjected to forces due to the cutting and to centrifugal movement, the inserts were fixed, joined to the base by a specific adhesive for metals; namely, a Loctite[®] 640 manufactured by Henkel Corporation (Henkel Corporation, Rocky Hill, CT, USA) [45]. In addition, to accelerate the glued process, the Loctite[®] 7471 (Henkel Corporation, Rocky Hill, CT, USA) curing activator was used [45].

The number of specimens manufactured was nine in total: three for each type of section and, for each one of them, another three for each material. For this study, only one of the specimens was used since, due to the small depth of the cut used in the trials and the low number of the planned tests, only 2.25 mm were removed from the radius of the specimen. Additionally, due to the number and location of the inserts, all of the specimens are balanced and have a similar behaviour during the turning.

3.2. Cutting Tools

For turning operations, two types of tool have been selected with the same geometry (Figure 3) but different kinds of coating (Figure 4): specifically, two tools from SECO (SECO Tools, Björnbacksvägen, Fagersta, Sweden) called HX and CP200. HX is uncoated, and it is designed mainly for the machining of cast iron, stainless steels, and hardened steels, although it is also suitable for non-ferrous materials, such as aluminium and magnesium. CP200 is coated ((Ti, Al)N + TiN), and it is intended for finishing operations on heat-resistant alloys based on nickel, cobalt, iron, and titanium, but also for stainless steels.

**Figure 3.** Turning tool geometry and dimensions.

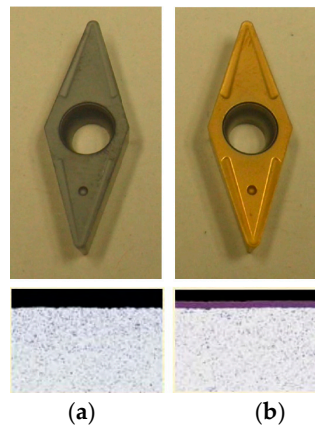


Figure 4. Types of coatings SECO used in tests called (a) HX; and (b) CP200.

This selection was made with the intention that the selected tools can be used to machine the largest possible number of material combinations, since, as noted above, this study is included in a research project of greater scope in which different material combinations were tested.

3.3. Cutting Conditions

To carry out the trials, a conventional horizontal lathe, Pinacho Model L1/200 (Pinacho, Huesca, Spain), was used (Figure 5). The choice of the values of the factors' levels for feed rate, f , spindle speed, S , and depth of cut, d , was conducted looking into the lathe's features, the values usually used during repair and maintenance operations, and the values which were easy to set on the machine to reduce, as far as possible, the probability of incurring operating errors. Thus, they were selected as follows: for f : 0.10 mm/rev and 0.15 mm/rev; for S : 925 rpm and 1470 rpm; and for d : 0.25 mm.



Figure 5. Pinacho Model L1/200 lathe.

3.4. Measurement Locations

All roughness measurements were taken with a Mitutoyo Surftest SJ 401 roughness tester (Mitutoyo America Corporation, Aurora, IL, USA) (Figure 6a). As noted above, the measurement locations along the specimen and regarding the inserts were taken as influential factors. These factors are the *LRS* and *LRI*. For the *LRS*, two values were taken: *LRS1*, roughness at the beginning of the specimen, and *LRS2*, roughness at the end of the specimen along the feeding direction. Specifically, *LRS1* was taken within the first 15 mm of the specimen and *LRS2* was taken within the last 15 mm of the specimen (Figure 6b). For the *LRI*, three levels were established according to the turning direction: *LRI1*, roughness before the insert, *LRI2*, roughness on the insert, and *LRI3*, roughness after the insert.

LRI2 was established along the generatrix located at the center of the insert, and *LRI1* and *LRI3* were established along two generatrix separated by 17.5° and -17.5° from the first one, respectively (Figure 6c).

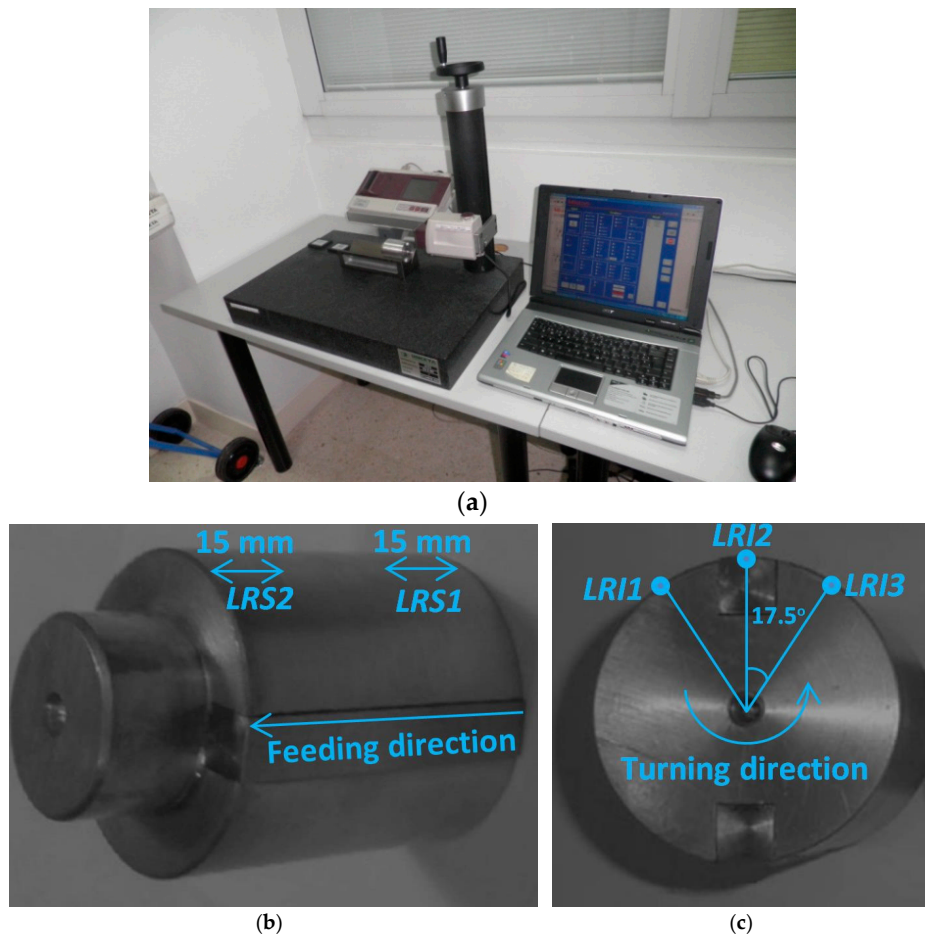


Figure 6. (a) Mitutoyo Surftest SJ 401 roughness tester; (b) the location of the measurements along the feeding direction; and (c) the location of the measurements according the turning direction.

3.5. Factors and Levels Selected

Table 4 shows, as a summary, the values selected for the different levels of each one of the factors analysed in this study.

Table 4. Selected values for the levels of each factor analysed.

Factors	Levels Values
Feed rate, <i>f</i> , (mm/rev)	0.10/0.15
Spindle speed, <i>S</i> , (rpm)	925/1470
Depth of cut, <i>d</i> , (mm)	0.25
Type of tool, <i>T</i>	HX/CP200
Location respect of the specimen, <i>LRS</i>	Beginning of the specimen/End of the specimen
Location respect of the insert, <i>LRI</i>	Before the insert/On the insert/After the insert

4. Results, Analysis, and Discussion

4.1. Results

After carrying out all of the turning tests, the roughness values in terms of the arithmetic mean deviation, Ra , were collected. The results obtained during the turning tests are found in Table 5.

Table 5. Values of the arithmetic mean deviation roughness, Ra (μm), obtained during turning tests.

No.	Test	Position	Ra , (μm)		Observations
			LRS1	LRS2	
1	HX_01_TP_P025_V150_A015	LRI2	0.86	0.86	1
		LRI1	0.88	0.93	2
		LRI3	1.09	0.99	3
2	HX_01_00_P025_V150_A010	LRI3	0.61	0.61	4
		LRI2	0.49	0.48	5
		LRI1	0.62	0.53	6
3	HX_02_TP_P025_V230_A010	LRI2	0.47	0.53	7
		LRI1	0.51	0.58	8
		LRI3	0.59	0.56	9
4	CP200_01_TP_P025_V150_A010	LRI3	0.56	0.58	10
		LRI2	0.45	0.43	11
		LRI1	0.58	0.60	12
5	CP200_01_00_P025_V230_A015	LRI3	1.08	0.96	13
		LRI2	0.78	0.78	14
		LRI1	0.84	0.83	15
6	HX_02_00_P025_V230_A015	LRI3	1.10	1.04	16
		LRI1	0.94	0.91	17
		LRI2	0.90	0.92	18
7	CP200_02_TP_P025_V150_A015	LRI1	0.96	0.92	19
		LRI2	0.84	0.93	20
		LRI3	1.13	1.26	21
8	CP200_02_00_P025_V230_A010	LRI1	0.52	0.56	22
		LRI2	0.43	0.50	23
		LRI3	0.56	0.47	24

Before carrying out a detailed statistical analysis of the results obtained in the present work, a first assessment was made to see if they followed any trend and, if so, if it was consistent with the results obtained in previous works in which the materials were studied separately. The results of this assessment are as follows:

- In relation to the feed rate, the values of the roughness increase in the three measured zones. Specifically, for $f = 0.10$ mm/rev, the mean values of the roughness are $Ra_{LRI1} = 0.57$ μm ; $Ra_{LRI2} = 0.48$ μm ; and $Ra_{LRI3} = 0.57$ μm , and for $f = 0.15$ mm/rev, the mean values of the roughness are $Ra_{LRI1} = 0.91$ μm ; $Ra_{LRI2} = 0.86$ μm ; and $Ra_{LRI3} = 1.08$ μm .
- With respect to the spindle speed, the values of Ra decrease slightly in the magnesium base and remain equal, or slightly increase, in the aluminum insert. Specifically, for $S = 925$ rpm, the mean values of the roughness are $Ra_{LRI1} = 0.76$ μm ; $Ra_{LRI2} = 0.67$ μm ; and $Ra_{LRI3} = 0.86$ μm . For $S = 1470$ rpm, the mean values of the roughness are $Ra_{LRI1} = 0.72$ μm ; $Ra_{LRI2} = 0.67$ μm ; and $Ra_{LRI3} = 0.80$ μm .

The results obtained in this work are coherent with those of other previous works about magnesium [55–61] and aluminum [47–53]. The magnesium works were of continuous and intermittent

horizontal turning and of continuous facing. In the horizontal turning, values of the roughness, Ra , increase with the feed rate values (0.40 μm and 0.60 μm for feed rate values of 0.05 mm/rev and 0.10 mm/rev, respectively), and slightly decrease with the spindle speed (0.53 μm and 0.50 μm for spindle speed values of 500 rpm and 800 rpm, respectively). In the facing trials, the same results occurred [39,41]. The values of the roughness, Ra , increased with the feed rate values (0.40 μm and 0.70 μm for the feed rate values of 0.08 mm/rev and 0.12 mm/rev, respectively) and decreased with the spindle speed (0.50 μm and 0.45 μm for spindle speed values of 500 rpm and 800 rpm, respectively). Regarding aluminium, this was done by horizontal turning, and it gave increasing Ra values with the feed rate and the spindle speed (0.47 μm and 0.70 μm for feed rate values of 0.05 mm/rev and 0.10 mm/rev, respectively, and 0.44 μm and 0.73 μm for spindle speeds of 150 rpm and 300 rpm, respectively) [47–53].

4.2. Statistical Discussion

Once the roughness values were obtained during the turning tests, a fixed effects ANOVA analysis was conducted over the obtained values of roughness, Ra , considering third-order interactions and eliminating a factor if its p -value was greater than 0.05. The final result for the statistically significant factors is shown in Table 6.

Table 6. ANOVA results for Ra Naperian logarithm.

Source	Degrees of Freedom	Sum of Squares	Mean Square	F	Pr > F
S	1	0.022	0.022	5.57	0.023
f	1	3.920	3.920	972.28	<0.001
LRI	2	0.340	0.170	42.20	<0.001
f^*LRI	2	0.063	0.032	7.86	0.001
T^*S	2	0.043	0.021	5.27	0.009
Error	39	0.157	0.004	-	-
Total	47	4.546	-	-	-

When the hypotheses on the residuals of the model were checked on the response variable Ra , there was evidence of a lack of normality and a lack of heterocedasticity. Due to this fact, carrying out a transformation of the roughness data was necessary. Logarithmic transformation of the response variable is simple and preserves the order of the original roughness data. Thus, a Naperian logarithmic transformation was applied on the Ra data and an ANOVA analysis was conducted, finding no evidence in this new variable a lack of either normality or heteroscedasticity, or the existence of any pattern in the model. The checking of these hypotheses can be observed in Table 7 and in Figure 7, respectively.

For each factor, the last column in Table 6 contains the probability for which a Snedecor's F distribution, with the degrees of freedom included in the column DF, achieves a value higher than the F value calculated. If this probability is higher than 0.05 (p -value > 0.05), it was considered that the effect corresponding to this factor was not statistically significant.

Table 7. Tests for normality on residuals associated with the Table 6 model.

Test for Normality	Statistic	p -Value
Kolmogorov–Smirnov	D	0.0678
Cramer–von Mises	W-Sq	0.0332
Anderson–Darling	A-Sq	0.2486

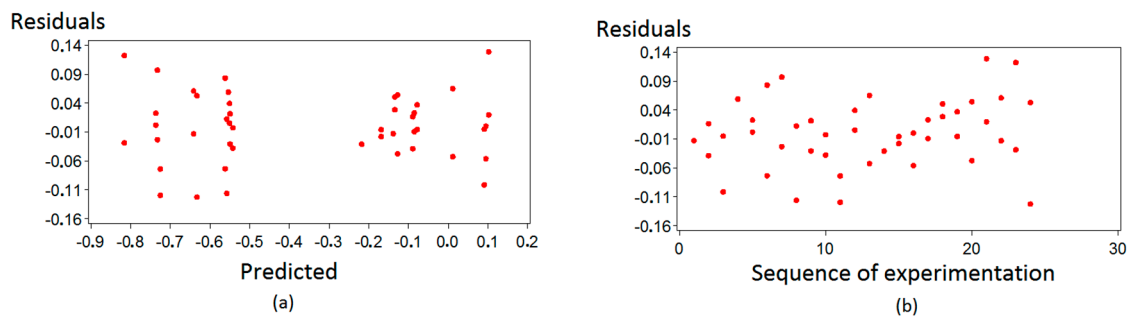


Figure 7. Checking of (a) the homoscedasticity hypothesis and (b) the non-existence of patterns on residuals of the associated Table 6 model.

In view of the ANOVA results, it is possible to conclude that the feed, f , very prominently and, to a lesser extent, the location with respect to the insert, LRI , the interaction feed rate*location with respect to the insert, $f*LRI$, the interaction type of the tool*spindle speed, $T*S$, and the spindle speed, S , significantly influence the resulting surface roughness of the turning hybrid components based on magnesium alloys. In fact, 86% of the variability in the surface roughness is due to the feed rate, which is the most influential parameter. Followed by the position with respect to the insert (7.49%), the other three sources of variation made a very small contribution (Table 8). The location with respect to the specimen, LRS , is not listed in Table 8, which means that the differences observed between the measured roughness at the beginning of the specimen and at the end of the specimen were not statistically significant.

Table 8. Contribution percentage for each factor.

Source	Contribution Percentage (%)
S	0.49
f	86.23
LRI	7.49
$f*LRI$	1.39
$T*S$	0.94
Total	96.54

Figure 8 illustrates the great influence of feed rate on the surface finish of the turning process and shows that the best results for surface finish are obtained for the lower feed rate tested (0.10 mm/rev). If this increases, the natural logarithm of the roughness ($\ln Ra$) increases rapidly and, therefore, the roughness surface also increases. This result agrees with the results of other experimental studies on turning processes [27,48].

In Figure 9, it can be appreciated how the surface roughness varies regarding the location with respect to the insert. A better surface roughness is observed on the insert than before or after it.

The interaction between the feed rate and the location with respect to the insert, $f*LRI$, is graphically illustrated in Figure 10. For the feed rate of 0.10 mm/rev, there are no differences between the logarithm of the roughness before and after the insert, while they do exist when the feed rate increases, worsening the roughness after the insert in a larger proportion. However, when the feed rate is 0.15 mm/rev, there are no differences between the surface roughness before the insert and on the insert. Figure 11 shows the usefulness of interaction graphs. Since the three lines represented are not parallel, the model underlying the ANOVA analysis is not additive. Graphically, the moderating effect of LRI on the increase of the Ra roughness can be seen when the feed rate f augments it.

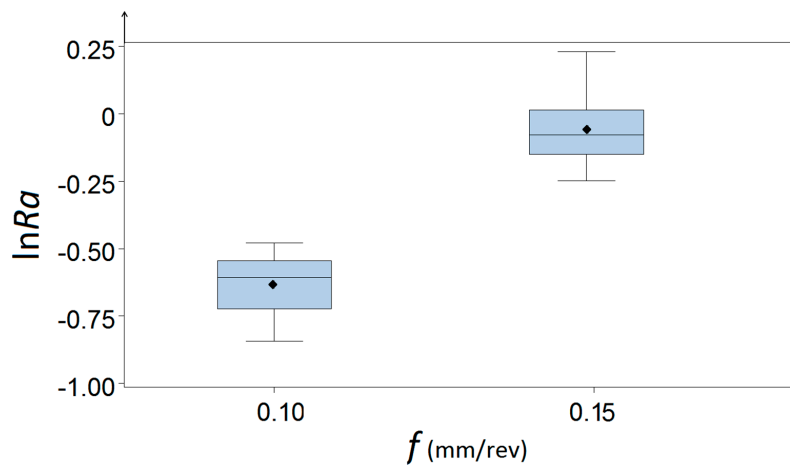


Figure 8. Box and whisker plot with dispersion of $\ln Ra$ with respect to the feed rate factor.

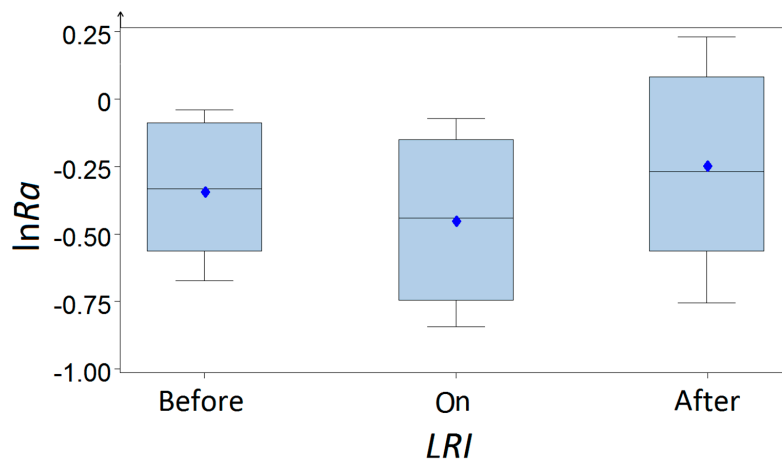


Figure 9. Box and whisker plot with the dispersion of $\ln Ra$ versus location with respect to the insert factor.

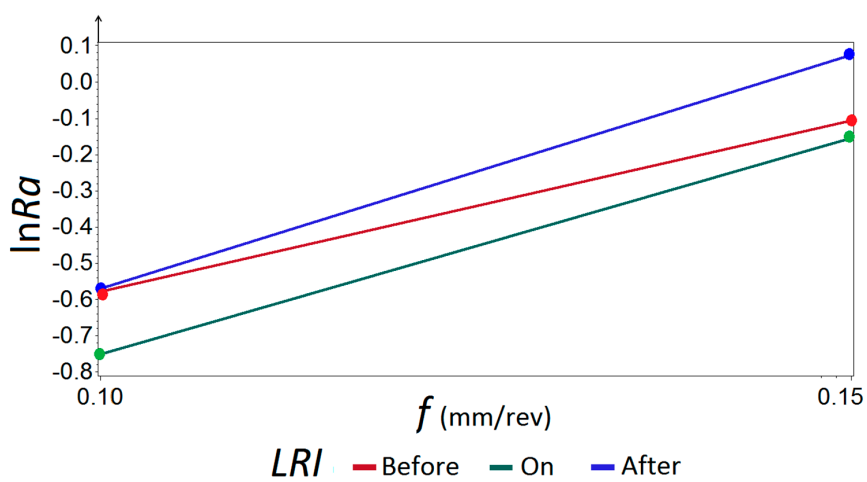


Figure 10. Interaction between the feed rate and location with respect to the insert for $\ln Ra$.

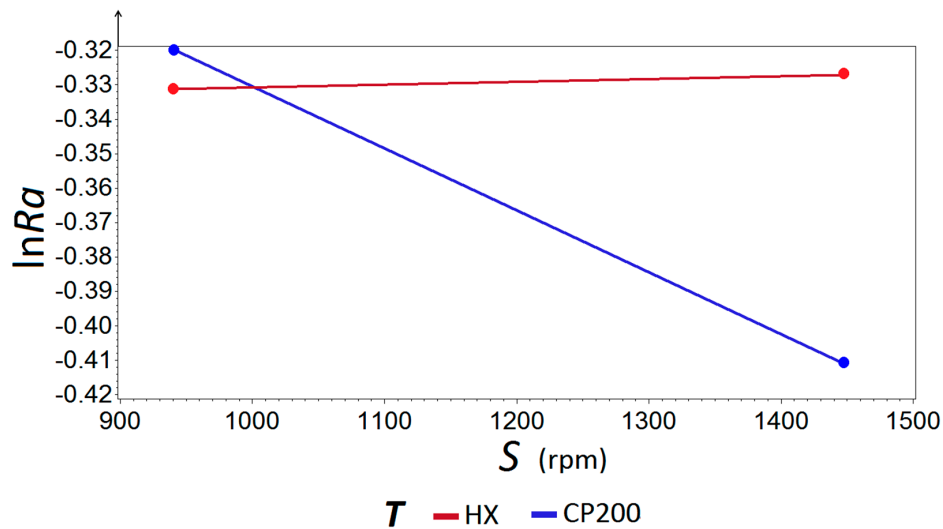


Figure 11. Interaction between the type of tool and the spindle speed for $\ln Ra$.

In Figure 11, the interaction between the type of tool and the spindle speed, $T \cdot S$, can be observed. The CP200 tool slightly improves the surface finish when the spindle speed increases, while the HX tool shows a more stable behaviour.

As a consequence of the obtained results, the variability of the surface roughness in the dry turning process is modeled through Equation (2):

$$Ra_{ijkl} = \exp(\mu + s_i + f_i + lri_k + f^*lri_{jk} + t^*s_{li} + \varepsilon_{ijkl}) \quad (2)$$

where s_i , f_i , γ_k , lri_k , f^*lri_{jk} , and t^*s_{li} represent the effect of the spindle speed, the feed rate, the location with respect to the insert, the interaction feed rate*location with respect to the insert, and the interaction of the type of tool*spindle speed, respectively. The hypothesis of such a model was contrasted through the residuals study, and no evidence of a lack of normality or heterocedasticity was found, nor the existance of patterns in the model.

The model of Equation (2) allows us to obtain the roughness values predicted by such a model for the different combinations of the parameter levels of the turning process. Table 9 shows the ranking for such combinations based on roughness predictions.

In Table 9, it is observed that the combination of the parameter levels that optimize the surface finish in the turning process, minimizing the prediction for Ra , is a feed of 0.10 mm/rev, a spindle speed of 1470 rpm, and the CP200 tool. Using such machining conditions, which are optimal for all of the superficial zones of the pieces, good levels of roughness are expected to be reached: about 0.42 μm on the insert and about 0.53 μm on the rest of the surface piece.

Table 9. Ranking of the combinations of the cutting conditions.

S , (rpm)	LRI	T	f , (mm/rev)	Prediction of Ra , (μm)
1470	On the insert	CP200	0.10	0.42
925	On the insert	CP200	0.10	0.46
925	On the insert	HX	0.10	0.46
1470	On the insert	HX	0.10	0.46
1470	Before the insert	CP200	0.10	0.53
1470	After the insert	CP200	0.10	0.53

Table 9. Cont.

<i>S</i> , (rpm)	<i>LRI</i>	<i>T</i>	<i>f</i> , (mm/rev)	Prediction of <i>Ra</i> , (µm)
925	Before the insert	CP200	0.10	0.57
925	Before the insert	HX	0.10	0.57
1470	Before the insert	HX	0.10	0.57
925	After the insert	CP200	0.10	0.58
925	After the insert	HX	0.10	0.58
1470	After the insert	HX	0.10	0.58
1470	On the insert	CP200	0.15	0.80
1470	Before the insert	CP200	0.15	0.84
925	On the insert	CP200	0.15	0.87
925	On the insert	HX	0.15	0.87
1470	On the insert	HX	0.15	0.87
925	Before the insert	CP200	0.15	0.92
925	Before the insert	HX	0.15	0.92
1470	Before the insert	HX	0.15	0.92
1470	After the insert	CP200	0.15	1.01
925	After the insert	CP200	0.15	1.10
925	After the insert	HX	0.15	1.10
1470	After the insert	HX	0.15	1.10

4.3. Technological Discussion

After discussing the results obtained during the statistical analysis of variance (ANOVA), and paying attention to the objective set out in this study, the practical application is discussed.

Due to the high cost of some parts used in the aeronautical sector, it is necessary to carry out repair and maintenance operations to return them to service or to keep them as spare parts. The main objective in this type of operation is to achieve parts with the dimensional and surface quality requirements specified in the design drawings, so that they can remain functional. In the aeronautical sector, the specified values that are usually given for surface roughness are within the range of $0.8 \mu\text{m} < Ra < 1.6 \mu\text{m}$ [72].

The surface roughness obtained in the tests carried out with the selected cutting conditions was in a range between $0.43 \mu\text{m}$ and $1.26 \mu\text{m}$. The best results were achieved using a feed rate of 0.10 mm/rev , a spindle speed of 1470 rpm , and the CP200 tool. It can be seen that, for the lowest value of the feed rate tested, the values obtained are low; that is, lower than those usually required in the aeronautical industry mentioned above. Therefore, whenever the drawing requirements allow it, the highest value of the feed rate can be used with the intention of reducing the machining time, and, with it, the associated costs, since the expected values are within the required range. The cutting conditions recommended to obtain efficient repairs in these components are a feed rate of 0.15 mm/rev , a spindle speed of 1470 rpm , and the CP200 tool. In addition, the wear of the tools is practically imperceptible in all cases analysed.

When observing the effect produced by the increase of the spindle speed in the behaviour of the CP200 tool, it is possible to think it would be good to increase the feed rate and the spindle speed in order to try to reduce the machining time and, with it, the repair time. Therefore, it is proposed that performing more turning trials to confirm that the *Ra* values obtained with the new higher values of feed rate and spindle speed continue to be within the usual range required for aeronautical applications, and that the tools do not suffer severe wear, as in the case of the trials carried out in the present work (since, if that wear occurred, it would be necessary to change the tools and, therefore, the saved costs by reducing machining time would be counteracted by the need to change the tools).

From an environmental point of view, we emphasize the importance of having all tests carried out in dry conditions, that is, without using any type of lubricant or other cooling system. This not only allows for the reduction of costs during repair/maintenance operations, but also makes

these operations compatible and sustainable with the environment while maintaining the surface roughness required.

5. Conclusions

The experimental study of the turning process on metallic hybrid components with a base UNS M11917 magnesium alloy and inserts of UNS A92024 aluminium alloy has confirmed that the surface finish is strongly influenced by the feed rate, the lowest values of feed rate proving to be more beneficial to the surface finish. The analysis of the interaction type of tool*spindle speed has allowed for an appreciable improvement in the surface roughness when the spindle speed is increased and the hybrid specimen is machined with the tool CP200. The analysis of the interaction feed rate*location with respect to the insert shows how the surface roughness becomes worse when the feed rate is increased, especially after the insert. Furthermore, the differences observed between measuring the roughness at the beginning of the component and measuring it at the end of the component are not statistically significant. Taking into consideration the surface roughness values usually required in the aeronautical sector and among the set of factors selected in this study, a feed rate of 0.15 mm/rev, a spindle speed of 1470 rpm, a CP200 tool, and dry machining are the best conditions to carry out repair operations efficiently and in an environmentally sustainable manner. It has also been seen that it is possible that there are some other combinations of the parameters that allow for an improvement of the results obtained in this work (in terms of reducing machining time and costs) increasing, simultaneously, the values of the feed rate and the spindle speed.

Acknowledgments: The authors thank the Research Group of the UNED “Industrial Production and Manufacturing Engineering (IPME)” for the support given during the development of this work, which has been financed in part by six grants from Ministerio de Ciencia e Innovación, Ministerio de Economía y Competitividad, Agencia Estatal de Investigación (AEI), Fondo Europeo de Desarrollo Regional (FEDER), and Industrial Engineering School-UNED (DPI2014-58007-R, MTM2016-78227-C2-1-P, MTM2015-69323-REDT, MTM2013-46374-P, CGL2014-58322-R and REF2018-ICF05), Spain. The authors also thank the Antolín Group for the material provided.

Author Contributions: Eva María Rubio, María Villeta, José Luis Valencia, and José Manuel Sáenz de Pipaón conceived and designed the experiments; Eva María Rubio and José Manuel Sáenz de Pipaón performed the experiments; Eva María Rubio, María Villeta, José Luis Valencia, and José Manuel Sáenz de Pipaón analysed the data; Eva María Rubio and José Manuel Sáenz de Pipaón contributed materials; María Villeta and José Luis Valencia contributed analysis tools; and Eva María Rubio, María Villeta, José Luis Valencia, and José Manuel Sáenz de Pipaón wrote the paper.

Conflicts of Interest: The authors declare no conflict of interest.

References

1. Ashby, M.F.; Brécht, Y.J.M. Designing hybrid materials. *Acta Mater.* **2003**, *51*, 5801–5821. [[CrossRef](#)]
2. Kickelbickm, G. *Hybrid Materials. Synthesis, Characterization and Applications*; Wiley-VCH Verlag GmbH & Co.: Darmstadt, Germany, 2007; ISBN 978-3-527-31299-3.
3. Zakaria, B.; Yazid, H. Friction stir welding of dissimilar materials Aluminum Al6061-T6 to ultra low carbon steel. *Metals* **2017**, *7*, 42. [[CrossRef](#)]
4. Casalino, G. Advances in welding metal alloys, Dissimilar metals and additively manufactured parts. *Metals* **2017**, *7*, 32. [[CrossRef](#)]
5. Casalino, G.; Guglielmi, P.; Lorusso, V.D.; Mortello, M.; Peyre, P.; Sorgente, D. Laser offset welding of AZ31B magnesium alloy to 316 stainless steel. *J. Mater. Process. Technol.* **2017**, *242*, 49–59. [[CrossRef](#)]
6. Li, Y.; Liu, C.; Yu, H.; Zhao, F.; Wu, Z. Numerical simulation of Ti/Al bimetal composite fabricated by explosive welding. *Metals* **2017**, *7*, 407. [[CrossRef](#)]
7. Cui, X.; Wang, S.; Hu, S.J. A method for optimal design of automotive body assembly using multi-material construction. *Mater. Des.* **2008**, *29*, 381–387. [[CrossRef](#)]
8. Gururaja, M.N.; Rao, A.N.H. A review on recent applications and future prospectus of hybrid composites. *Int. J. Soft Comput. Eng.* **2012**, *1*, 352–355.

9. Lee, D.; Morillo, C.; Oller, S.; Bugeda, G.; Oñate, E. Robust design optimization of advance hybrid (fiber-metal) composite structures. *Compos. Struct.* **2013**, *99*, 181–192. [[CrossRef](#)]
10. DRL. *Innovation Report 2011*; Institute of Composites Structures and Adaptative Systems: Braunschweig, Germany, 2011.
11. Wagner, F.; Zerner, I.; Kreimeyer, M.; Seefeld, T.; Sepold, G. Characterization and properties of dissimilar metal combinations of Fe/Al and Ti/Al sheet materials. In Proceedings of the ICALEO'01, Orlando, FL, USA, 15–18 October 2001.
12. Luo, J.G.; Acoff, V.L. Interfacial reactions of titanium and aluminum during diffusion welding. *Weld. J.* **2000**, *79*, 239s–243s.
13. Dau, J.; Lauter, C.; Damerow, U.; Homberg, W.; Tröster, T. Multi-material systems for tailored automotive structural components. In Proceedings of the 18th International Conference on Composite Materials, Jeju Island, Korea, 21–26 August 2011.
14. Amancio, S. *Innovative Solid-State Spot Joining Methods for Fiber Composites and Metal-Polymer Hybrid Structures; Joining in Car Body*; Helmholtz-Zentrum Geesthacht: Geesthacht, Germany, 2012; pp. 1–47.
15. Frantz, M.; Lauter, C.; Tröster, T. Advanced manufacturing technologies for automotive structures in multi-material design consisting of high-strength steels and CFRP. In Proceedings of the 56th International Scientific Colloquium, Ilmenau, Germany, 12–16 September 2011.
16. Suryawanshi, B.K.; Prajitsen, G.D. Review of design of hybrid aluminum/composite drive shaft for automobile. *Int. J. Innov. Technol. Explor. Eng.* **2013**, *2*, 259–266.
17. Uthayakumar, M.; Prabhakaran, G.; Aravindan, S.; Sivaprasad, J.V. Machining studies on bimetallic piston with CBN tool using the Taguchi method-technical communication. *Mach. Sci. Technol.* **2008**, *12*, 249–255. [[CrossRef](#)]
18. Goede, M.; Stehlin, M.; Rafflenbeul, L.; Kopp, G.; Beeh, E. Super light car: Lightweight construction thanks to a multi-material design and functional integration. *Eur. Transp. Res. Rev.* **2009**, *1*, 5–10. [[CrossRef](#)]
19. Ben-Artzy, A.; Munitz, A.; Kohn, G.; Bronfin, B.; Shtechman, A. Joining of light hybrid constructions made of magnesium and aluminum alloys. *Magn. Technol.* **2002**, 295–302. [[CrossRef](#)]
20. Sáenz de Pipaón, M.J. Diseño y Fabricación de Probetas de Componentes Híbridos con Aleaciones de Magnesio para Ensayos de Mecanizado. Ph.D. Thesis, UNED (Universidad Nacional de Educación a Distancia), Madrid, Spain, 2013.
21. Qi, X.; Song, G. Interfacial structure of the joints between magnesium alloy and mild steel with nickel as interlayer laser-TIG welding. *Mater. Des.* **2010**, *31*, 605–609. [[CrossRef](#)]
22. Nasiri, A.M.; Li, L.; Kim, S.H.; Zhou, Y.; Weckman, D.C.; Nguyen, T.C. Microstructure and properties of laser brazed magnesium to coated steel. *Weld. J.* **2011**, *90*, 211s–219s.
23. Nasiri, A.M.; Weckman, D.C.; Zhou, Y. Interfacial microstructure of diode laser brazed AZ31B magnesium to steel sheet using a nickel interlayer. *Weld. J.* **2013**, *92*, 1–10.
24. Krebs, R.; Böhme, J.; Doerr, J.; Rothe, A.; Schneider, W.; Haberling, C. Magnesium, hybrid turbo engine from Audi. *MTZ Worldw.* **2005**, *66*, 13–16. [[CrossRef](#)]
25. Fischersworing-Bunk, A.; Landerl, C.; Fent, A.; Wolf, J. The new BMW inline six-cylinder composite Mg/Al crankcase. In Proceedings of the IMA 05, 62nd Annual World Magnesium Conference, Berlin, Germany, 22–24 May 2005.
26. Carou, D.; Rubio, E.M.; Davim, J.P. Analysis of ignition risk in intermittent turning of UNS M11917 magnesium alloy at low cutting speeds based on the chip morphology. *Proc. Inst. Mech. Eng. Part B J. Eng. Manuf.* **2015**, *229*, 365–371. [[CrossRef](#)]
27. Sáenz de Pipaón, M.J.; Rubio, E.M.; Villeta, M.; Sebastián, M.A. Influence of cutting conditions and tool coatings on the surface finish of workpieces of magnesium obtained by dry turning. In Proceedings of the 19th International DAAAM Symposium, Trnava, Slovakia, 22–25 October 2008; pp. 604–605.
28. Bisker, J.; Christman, T.; Allison, T.; Goranson, H.; Landmesser, J.; Minister, A.; Plonski, R. *DOE Handbook, Primer on Spontaneous Heating and Pyrophoricity*; U.S. Department of Energy: Washington, DC, USA, 1994; pp. 1–68.
29. NanoMAG. *Hydro Magnesium's Machining Magnesium*; Technical Document; NanoMAG: Livonia, MI, USA, 2009; Available online: <http://nanomag.us> (accessed on 22 November 2017).

30. Rubio, E.M.; Sáenz de Pipaón, M.J.; Villeta, M.; Sebastián, M.A. Experimental study for improving repair operations of pieces of magnesium UNS M11311 obtained by dry turning. In Proceedings of the 12th CIRP Conference on Modelling of Machining, San Sebastian, Spain, 7–8 May 2009; pp. 819–826.
31. Carou, D.; Rubio, E.M.; Davim, J.P. Discontinuous cutting: Failure mechanisms, tools materials and temperature study—A review. *Rev. Adv. Mater. Sci.* **2014**, *38*, 110–124.
32. Rubio, E.M.; de Agustina, B.; Marín, M.M.; Bericua, A. Cooling systems based on cold compressed air: A review of the applications in machining processes. *Proc. Eng.* **2015**, *132*, 413–418. [[CrossRef](#)]
33. Carou, D.; Rubio, E.M.; Davim, J.P. A note on the use of the minimum quantity lubrication (MQL) system in turning. *Ind. Lubr. Tribol.* **2015**, *67*, 256–261. [[CrossRef](#)]
34. Arokiadass, R.; Palaniradja, K.; Alagumoorthi, N. Effect of process parameters on surface roughness in end milling of Al/SiCp MMC. *Int. J. Eng. Sci. Technol.* **2011**, *13*, 276–284.
35. Carou, D.; Rubio, E.M.; Lauro, J.P.; Davim, J.P. Experimental investigation on surface finish during intermittent turning of UNS M11917 magnesium alloy under dry and near dry machining conditions. *Measurement* **2014**, *56*, 136–154. [[CrossRef](#)]
36. Carou, D.; Rubio, E.M.; Lauro, J.P.; Davim, J.P. Experimental investigation on finish intermittent turning of UNS M11917 magnesium alloy under dry machining. *Int. J. Adv. Manuf. Technol.* **2014**, *75*, 1417–1429. [[CrossRef](#)]
37. Ozsváth, P.; Szmejkál, A.; Takács, J. Dry milling of magnesium based hybrid materials. *Transp. Eng.* **2008**, *36*, 73–78. [[CrossRef](#)]
38. Prakash, S.; Palanikumar, K.; Mercy, J.L.; Nithyalakshmi, S. Evaluation of surface roughness parameters (Ra, Rz) in drilling of MDF composite panel using Box-Behnken experimental design (BBD). *Int. J. Des. Manuf. Technol.* **2011**, *5*, 52–62.
39. Rubio, E.M.; Valencia, J.L.; Saá, A.J.; Carou, D. Experimental study of the dry facing of magnesium pieces based on the surface roughness. *Int. J. Precis. Eng. Manuf.* **2013**, *14*, 995–1001. [[CrossRef](#)]
40. Rubio, E.M.; Villeta, M.; Carou, D.; Saá, A.J. Comparative analysis of sustainable cooling systems in intermittent turning of magnesium pieces. *Int. J. Precis. Eng. Manuf.* **2014**, *15*, 929–940. [[CrossRef](#)]
41. Rubio, E.M.; Valencia, J.L.; de Agustina, B.; Saá, A.J. Tool selection based on surface roughness in dry facing repair operations of magnesium pieces. *Int. J. Mater. Prod. Technol.* **2014**, *48*, 116–134. [[CrossRef](#)]
42. Sáenz de Pipaón, J.M.; Rubio, E.M.; Villeta, M.; Sebastián, M.A. Analysis of the chips obtained by dry turning of UNS M11311 magnesium. In Proceedings of the 3rd Manufacturing Engineering Society International Conference 2009, Alcoy, Spain, 17–19 June 2009; pp. 33–38.
43. Sáenz de Pipaón, J.M.; Rubio, E.M.; Villeta, M.; Sebastián, M.A. Selection of the cutting tools and conditions for the low speed turning of bars of magnesium UNS M11311 based on the surface roughness. In *Innovative Production Machines and Systems*; Whittles Publishing: Scotland, UK, 2010; pp. 174–179, ISBN 978-184995-006-0.
44. Villeta, M.; Rubio, E.M.; Sáenz de Pipaón, J.M.; Sebastián, M.A. Surface finish optimization of magnesium pieces obtained by dry turning based on Taguchi techniques and statistical test. *Mater. Manuf. Process.* **2011**, *26*, 1503–1510. [[CrossRef](#)]
45. Rubio, E.M.; Sáenz de Pipaón, J.M.; Valencia, J.L.; Villeta, M. *Design, Manufacturing and Machining Trials of Magnesium Based Hybrid Parts, Machining of Light Alloys: Aluminium, Titanium and Magnesium*; CRC-Press: Boca Raton, FL, USA, 2018; under review.
46. Montgomery, D.C. *Design and Analysis of Experiments*; John Wiley & Sons, Inc.: New York, NY, USA, 2005.
47. Rubio, E.M.; Camacho, A.M.; Sánchez, J.M.; Marcos, M. Surface roughness of AA7050 alloy turned bars, analysis of the influence of the length of machining. *J. Mater. Process. Technol.* **2005**, *162–163*, 682–689. [[CrossRef](#)]
48. Batista, M.; Sánchez-Carrilero, M.; Rubio, E.M.; Marcos, M. *Cutting Speed and Feed Based Analysis of Chip Arrangement in the Dry Horizontal Turning of UNS A92024 Alloy*; Annals of the DAAAM for 2009; DAAAM International: Vienna, Austria, 2009; Volume 20, pp. 967–968. ISBN 978-3-901509-70-4.
49. Saá, A.J.; Agustina, B.; Marcos, M.; Rubio, E.M. Experimental study of dry turning of UNS A92024-T3 aluminium alloy bars based on surface roughness. *AIP Conf. Proc.* **2009**, *1181*, 151–158.
50. Agustina, B.; Saá, A.; Marcos, M.; Rubio, E.M. Analysis of the machinability of aluminium alloys UNS A97050-T7 and UNS A92024-T3 during short dry turning tests. *Adv. Mater. Res.* **2011**, *264–265*, 931–936. [[CrossRef](#)]

51. Agustina, B.; Rubio, E.M. Experimental study of cutting forces during dry turning processes of UNS A92024-T3 aluminium alloys. In Proceedings of the 4th Manufacturing Engineering Society International Conference 2011 (MESIC 2011), Cadiz, Spain, 21–23 September 2011; pp. 1–6.
52. Agustina, B.; Rubio, E.M. Analysis of cutting forces during dry turning processes of UNS A92024-T3 aluminium bars. *Adv. Mater. Res.* **2012**, *498*, 25–30. [[CrossRef](#)]
53. Agustina, B.; Rubio, E.M.; Sebastian, M.A. Surface roughness model based on force sensors for the prediction of the tool wear. *Sensors* **2014**, *4*, 6393–6408. [[CrossRef](#)] [[PubMed](#)]
54. Villeta, M.; de Agustina, B.; Sáenz de Pipaón, J.M.; Rubio, E.M. Efficient optimisation of machining processes based on technical specifications for surface roughness: Application to magnesium pieces in the aerospace industry. *Int. J. Adv. Manuf. Technol.* **2012**, *60*, 1237–1246. [[CrossRef](#)]
55. Rubio, E.M.; Valencia, J.L.; Carou, D.; Saá, A.J. Inserts selection for intermittent turning of magnesium pieces. *Appl. Mech. Mater.* **2012**, *217–219*, 1581–1591. [[CrossRef](#)]
56. Rubio, E.M.; Villeta, M.; Saá, A.J.; Carou, D. Analysis of main optimization techniques in predicting surface roughness in metal cutting processes. *Appl. Mech. Mater.* **2012**, *217–219*, 2171–2182. [[CrossRef](#)]
57. Rubio, E.M.; Villeta, M.; Agustina, B.; Carou, D. Surface roughness analysis of magnesium pieces obtained by intermittent turning. *Mater. Sci. Forum* **2014**, *773–774*, 377–391. [[CrossRef](#)]
58. Carou, D.; Rubio, E.M.; Lauro, C.H.; Davim, J.P. The effect of minimum quantity lubrication in the intermittent turning of magnesium based on vibration signals. *Measurement* **2016**, *94*, 338–343. [[CrossRef](#)]
59. Carou, D.; Rubio, E.M.; Lauro, C.H.; Brandão, L.C.; Davim, J.P. Study based on sound monitoring as a means for superficial quality control in intermittent turning of magnesium workpieces. *Procedia CIRP* **2017**, *62*, 262–268. [[CrossRef](#)]
60. Carou, D.; Rubio, E.M.; Davim, J.P. Chapter 5. Machinability of magnesium and its alloys: A review. In *Traditional Machining Processes*; Springer: Berlin/Heidelberg, Germany, 2015; pp. 1–20.
61. Sanz, C.; Fuentes, E.; Gonzalo, O.; Bengoetxea, I.; Obermair, F.; Eidenhammer, M. Advances in the ecological machining of magnesium and magnesium-based hybrid parts. *Int. J. Mach. Mach. Mater.* **2008**, *4*, 302–319. [[CrossRef](#)]
62. Fletcher, D.I.; Kapoor, A.; Steinhoff, K.; Schulteit, N. Theoretical analysis of steady-state texture formation during wear of a bi-material surface. *Wear* **2001**, *251*, 1332–1336. [[CrossRef](#)]
63. Sathesh, J.; Tajamul, P.; Madhusudhan, T.H. Optimal machining conditions for turning of AlSiC Metal Matrix Composites using ANOVA. *Int. J. Innov. Res. Sci. Eng. Technol.* **2013**, *2*, 6171–6176.
64. Sokolowsky, J.H.; Szablewski, D.; Kasprzak, W.; Ng, E.G.; Dumitrescu, M. Effect of tool cutter immersion on Al-Si bi-metallic materials in high-speed milling. *J. Achiev. Mater. Manuf. Eng.* **2006**, *17*, 15–20.
65. Vicario, I.; Crespo, I.; Plaza, L.M.; Caballero, P.; Idoaga, I.K. Aluminium Foam and Magnesium Compound Casting Produced by High-Pressure Die Casting. *Metals* **2016**, *6*, 24. [[CrossRef](#)]
66. Vilches, F.J.T.; Hurtado, L.S.; Fernandez, F.M.; Bermudo, C. Analysis of the chip geometry in dry machining of aeronautical aluminum alloys. *Appl. Sci.* **2017**, *7*, 132. [[CrossRef](#)]
67. Rafai, N.H.; Islam, M.N. An investigation into dimensional accuracy and surface finish achievable in dry turning. *Mach. Sci. Technol.* **2009**, *13*, 571–589. [[CrossRef](#)]
68. Rincon Troconis, B.C.; Frankel, G.S. Effects of Pretreatments on the Adhesion of Acetoacetate to AA2024-T3 Using the Blister Test. *Corrosion* **2014**, *70*, 483–495. [[CrossRef](#)]
69. Arokiasamy, S.; Anand Ronald, B. Experimental investigations on the enhancement of mechanical properties of magnesium-based hybrid metal matrix composites through friction stir processing. *Int. J. Adv. Manuf. Technol.* **2017**, *93*, 493–503. [[CrossRef](#)]
70. Grzesik, W. *Advanced Machining Processes of Metallic Materials: Theory, Modelling and Applications*; Elsevier: Amsterdam, the Netherlands, 2008.
71. Taub, A. Automotive materials: Technology trends and challenges in the 21st century. *MRS Bull.* **2006**, *31*, 336–343. [[CrossRef](#)]
72. The American Society of Mechanical Engineers. *Surface Texture: Surface Roughness, Waviness and Lay*; ANSI/ASME B46.1-2009; ASME: New York, NY, USA, 2010.

